Inception Length to a Fully Developed, Fin-Generated, Shock-Wave, Boundary-Layer Interaction

Frank K. Lu*
University of Texas at Arlington, Arlington, Texas 76019
and
Gary S. Settles†
Pennsylvania State University, University Park, Pennsylvania 16802

An experimental study of fin-generated, shock-wave, turbulent, boundary-layer interactions confirmed previous observations that, sufficiently far from the fin apex, such interactions become conical. For Mach numbers from 2.5 to 4 and fin angles from 4 to 22 deg, the inception length to conical symmetry was found to increase weakly with Mach number. Also, the inception length was found to depend primarily on the inviscid shock angle, this angle ranging from 21 to 40 deg. The inception length decreased with shock strength and was small (approximately constant at three boundary-layer thicknesses in length) at the largest shock strengths encountered.

Nomenclature

a, b = ⅓, constants in power of Re_δ in Reynolds-number scaling law, Eq. (3)
M_n = $M_\infty \sin \beta_0$, Mach number normal to the inviscid shock-wave trace on the test surface
M_∞ = incoming freestream Mach number
r, β = polar coordinate system centered at the virtual origin, Fig. 2b
Re_δ = Reynolds number based on the undisturbed boundary-layer thickness at the start of the interaction
α = angle made by fin with respect to the incoming freestream direction
β = angle made by surface-flow features with respect to the incoming freestream direction
$\Delta\beta_U$ = reduced upstream-influence angle, $(\beta_U - \mu_\infty)$
$\Delta\beta_0$ = reduced shock angle, $(\beta_0 - \mu_\infty)$
δ = undisturbed boundary-layer thickness at the start of the interaction
μ_∞ = Mach number of incoming freestream, $\sin^{-1} 1/M_\infty$
ξ, η, ζ = orthonormal coordinate system based on the inviscid shock-wave trace on the test surface, Fig. 2b

Subscripts

i = inception
U = upstream influence
0 = inviscid shock trace on test surface
∞ = incoming freestream conditions

Superscripts

$\bar{()}$ = normalized by δ
$\tilde{()}$ = nondimensionalization, Eq. (3)

Introduction

SHOCK-WAVE boundary-layer interactions form an important class of fluid dynamics problems because of their ubiquitous presence in high-speed flight. These interactions are conveniently divided into two-dimensional and three-dimensional types based on the geometry inducing the interaction. Three-dimensional interactions can be further classified into dimensional and dimensionless interactions.[1,2] Dimensional types have explicit geometrical length scales such as diameter or a thickness whereas dimensionless types, obviously, have no length scales except those due to the flow itself (such as δ).

One basic configuration producing a dimensionless interaction is a sharp-edged fin mounted on a flat plate. The fin, inclined at an angle α to an incoming stream of Mach number M_∞, generates a shock sweeping across an incoming turbulent boundary layer (Fig. 1). (The inviscid shock generated by the fin makes an angle of β_0 with the incoming stream.) This idealization represents practical configurations such as those found at fin-fuselage junctions or in supersonic engine inlets. Fin-generated interactions have been recently reviewed[1,2]; thus, the following review will be narrowed to the inception-length issue under examination.

In a viscous flow, the fin-generated shock wave represents an adverse pressure gradient that the boundary layer must overcome. The interaction between two essentially disparate flow phenomena, the shock wave and the boundary layer, starts at the upstream-influence line. The upstream influence is readily observed using surface-flow visualization.[3,4] An example of such a pattern is shown in Fig. 2a while its key features are identified in Fig. 2b. In surface-flow visualization, the upstream influence is detected by the onset of deflection of the incoming surface streaks.

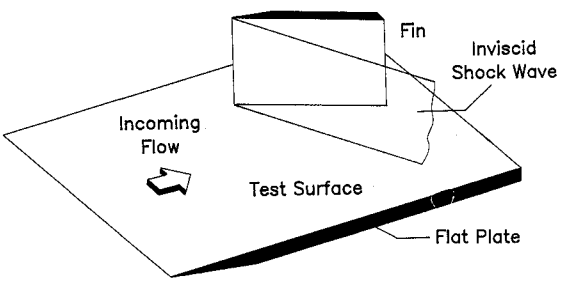

Fig. 1 Fin.

Received Aug. 9, 1989; revision received Feb. 27, 1990.

*Assistant Professor of Aerospace Engineering, UTA Box 19018. Member AIAA.
†Professor of Mechanical Engineering and Director, Gas Dynamics Laboratory. Associate Fellow AIAA.

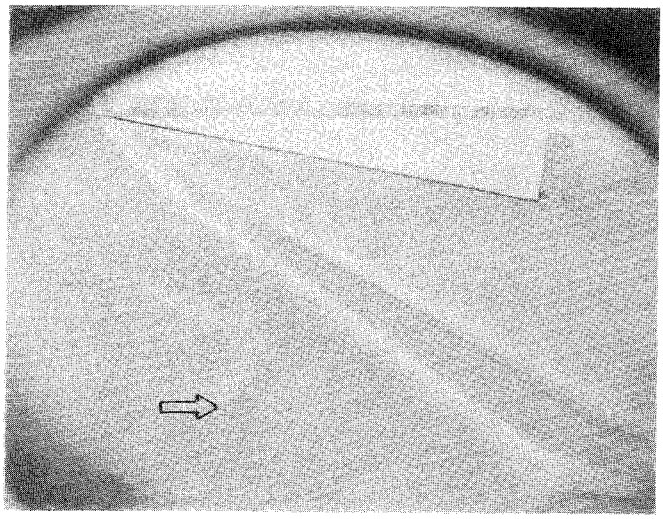

a) Example: $M_\infty = 2.95$, $\alpha = 15$ deg

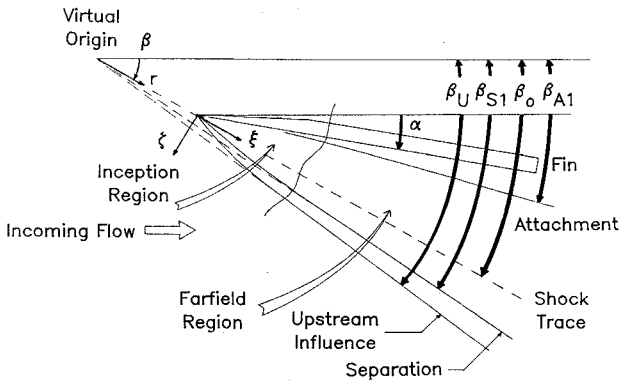

b) Sketch showing key surface features

Fig. 2 Surface-flow pattern in a fin-generated interaction.

The surface-flow pattern in a fin interaction shows an "inception region" near the fin leading edge and a far-field region further away (Fig. 2b).[5] Familiar examples of such near-field and far-field behavior include pipe inlet flows, wakes, and jets. In fin interactions, the surface features ahead of the inviscid shock in the far-field appear to radiate from a virtual origin, exhibiting "conical symmetry" (Fig. 2),[6] whereas in the region between the inviscid shock and the fin, conical symmetry is approximately valid. Cylindrical symmetry, on the other hand, occurs where the far-field interaction is parallel to the inviscid shock and can be found in other types of swept interactions such as those generated by certain swept compression corners.[1,5]

A natural coordinate system for the conical features in fin interactions is a polar coordinate system (r, β) centered at the virtual origin (see Fig. 2b). However, for convenience in data reduction and interpretation, a Cartesian coordinate system centered on the fin apex, with ξ along the inviscid shock trace, (ξ, ζ) may be used instead. The reason that the (ξ, ζ) coordinate system approximates the (r, β) system well is because the included angle $(\beta_U - \beta_0)$ is small, being typically less than 15 deg.

In the conical far field, a reduced upstream-influence angle $\Delta\beta_U$ scales with a reduced shock angle $\Delta\beta_0$, for $2.5 \le M_\infty \le 4$ and $0 \le \Delta\beta_0 \le 20$ deg, namely[7]:

$$\Delta\beta_U = 2.2\Delta\beta_0 - 0.027\Delta\beta_0^2 \tag{1}$$

For experiments where $\Delta\beta_0 < 5$ deg, the poorly resolved upstream influence line may give the impression of cylindrical symmetry. In addition, some measurements were performed inside the inception zone.[8,9] These experimental difficulties caused confusion over whether the interaction is conical or cylindrical, since most previous swept interaction studies were not meant to address this issue specifically. Lu et al.[7] also postulated that, at the large $\Delta\beta_0$ limit, $\Delta\beta_U \to \Delta\beta_0$, i.e., there would be cylindrical symmetry in this limiting situation. Experimental limitations, however, have thus far prevented observation of this behavior.

In a series of studies,[6,10-12] the spanwise development of the upstream influence was found to scale according to

$$\tilde{\zeta}_U/M_n = f(\tilde{\zeta}_U) \tag{2}$$

where

$$\tilde{\zeta}_U = (\zeta_U/\delta)Re_\delta^b \qquad \tilde{\zeta}_U = (\zeta_U/\delta)Re_\delta^a \tag{3}$$

Equation (2), with empirical constants $a = b = \frac{1}{3}$, was validated for Mach numbers from 2.5 through 4.[12] The cited reference identified the effect of the viscous parameters δ and Re_δ and the inviscid shock-strength parameter M_n on the upstream influence. Equation (2) also shows that M_n and the (ξ, ζ) coordinate system effectively account for α, the geometry parameter.

The inception point can be located at the departure of the upstream-influence line from its far-field asymptote. (Details on locating the inception point will be elaborated later.) At $M_\infty = 3$, Settles[13] found that

$$\tilde{\xi}_i \approx 1130 \cot\beta_0 \tag{4}$$

with $\tilde{\xi}_i = (\xi_i/\delta)Re_\delta^b$ being the nondimensional inception length according to Eq. (3). Experiments tailored to examine the far field should be performed outside this nondimensional inception region. Inger[14] found analytically that

$$\xi_i = C\zeta_i \cot\beta_0 \tag{5}$$

with the coefficient $C = \mathcal{O}(1)$ depending on Reynolds and Mach numbers, incoming boundary-layer profile, wall conditions, and shock-generator shape in general. Further, Eq. (2) implies a constant nondimensional value of $\tilde{\xi}_i$ that was given in Ref. 6 as

$$\tilde{\xi}_i \approx 1600 \tag{6}$$

The different inception length scaling of Eqs. (4) and (6) reflect the fact that the inception zone and the far field merge gradually so that the inception length may not be specified with high precision.

To broaden our understanding of fin-generated interactions, a study was recently completed covering a Mach number range from 2.5 through 4.[15] This paper presents results from that data base pertaining to the inception length, especially regarding its change with shock strength and Mach number.

Experimental Methods

Wind Tunnel and Test Models

The experiments were done in the Gas Dynamics Laboratory of the Pennsylvania State University using the Supersonic Wind Tunnel Facility. This facility is a blowdown wind tunnel with a test Mach number of 1.5 through 4, varied by an asymmetric sliding-block nozzle. The test section is 150 mm (6 in.) wide, 165 mm (6.5 in.) high, and 610 mm (24 in.) long. (Further description of the wind tunnel and the experiments can be found in Ref. 15.)

A flat plate 500 mm (19.5 in.) long, spanning the tunnel and mounted in the test section, provided the interaction test surface. On this plate was mounted a 10-deg sharp-edged fin serving as a shock generator. The fin was placed with its tip 216 mm (8.5 in.) from the plate leading edge and 26.2 mm (1.03 in.) from the tunnel sidewall. The fin was 100 mm (4 in.) high, 127 mm (5 in.) long, and 10.3 mm (0.404 in.) thick.

Table 1 Incoming freestream conditions

M_∞	p_0, MPa (psia)	T_0, K (°R)	$Re\ 10^{-6}$, m^{-1} (/ft)
2.47	0.54 ± 2.0% (78)	295 ± 0.9% (531)	53.8 ± 0.9% (16.3)
2.95	0.76 ± 2.7% (110)	295 ± 0.9% (531)	58.9 ± 1.9% (17.8)
3.44	1.03 ± 3.0% (150)	295 ± 0.8% (531)	64.0 ± 1.7% (19.4)
3.95	1.58 ± 5.0% (230)	295 ± 1.3% (531)	75.8 ± 1.7% (23.0)

Table 2 Boundary-layer parameters 216 mm (8.5 in.) from the flat-plate leading edge

M_∞	δ, mm	θ, mm	$c_f.10^3$	Π
2.47	3.4 ± 0.1	0.21 ± 0.03	1.76 ± 0.03	0.56 ± 0.07
2.95	3.2 ± 0.1	0.18 ± 0.05	1.62 ± 0.08	0.58 ± 0.11
3.44	3.3 ± 0.1	0.16 ± 0.05	1.54 ± 0.10	0.54 ± 0.09
3.95	3.2 ± 0.1	0.13 ± 0.03	1.41 ± 0.11	0.56 ± 0.10

The fin was held tightly onto the flat plate by a pneumatically driven rotation mechanism mounted on the tunnel sidewall. A rubber seal at the bottom of the fin prevented leaks from developing during the tests. The fin was rotated to a predetermined α, accurate to ± 0.1 deg, once test conditions were established. This was necessary only for tests with $\alpha \gtrsim 14$ deg, whereas at lower angles α was fixed before the run. In the experiments, α ranged from 4 to 22 deg, the largest value being limited by tunnel stall.

Test Conditions

The experiments were performed at M_∞ = 2.47, 2.95, 3.44, and 3.95 (Table 1). Since the wind tunnel is a blowdown type, the stagnation temperature T_0 decreased from 300 K (540°R) to 290 K (520°R) in a typical run of about 20 s. The nominal freestream unit Reynolds number Re was held relatively constant throughout the Mach number range at 50 to 75 × 10^6 m^{-1} (15 to 23 × 10^6/ft). In Table 1, the values of the test conditions and their standard deviations are not of "typical" runs but are obtained from the ensemble of runs of each Mach number throughout the test program. This is felt to provide a better characterization of the tests that were performed over an extended period.

The undisturbed boundary layers were two dimensional, turbulent, and in equilibrium at the test region and were approximately adiabatic. Some centerline boundary-layer parameters based on wall-wake curve fits at 216 mm (8.5 in.) from the flat-plate leading edge are listed in Table 2. No experimental data at M_∞ = 3.95 were available during this study, and those shown in the table are obtained by linear extrapolation of lower Mach number data. The validity of this extrapolation for turbulent, equilibrium, adiabatic boundary layers is discussed in Ref. 15.

Experimental Techniques and Data Analysis

The interaction surface was visualized by a kerosene-pigment dry-transfer technique.[3,4] Spatial data obtained from full-size undistorted images of the surface pattern (preserved on matte acetate tape) were, on average, resolved to 0.5 mm (0.02 in.) These data were digitized for subsequent analysis.

Figure 3 is an example of an upstream-influence line to illustrate the data analysis described later. Examination of the figure shows a slight bulge to the upstream-influence line within the inception region. (Notice also the bulge in the separation line in Fig. 2a.) This feature is particularly obvious in weakly separated interactions and was first observed by Stalker[16] and, more recently, by Özcan and Kaya[17] in swept step interactions. There are no satisfactory explanations as yet for this phenomenon. However, Özcan and Kaya suggest that this bulge occurs when M_n is just over unity so that the shock

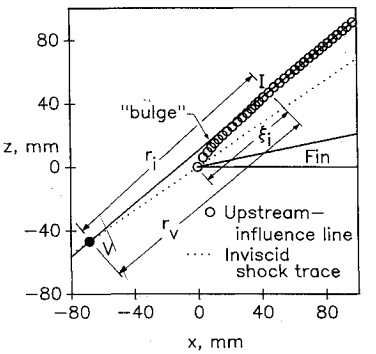

Fig. 3 Example: M_∞ = 2.47, α = 12 deg.

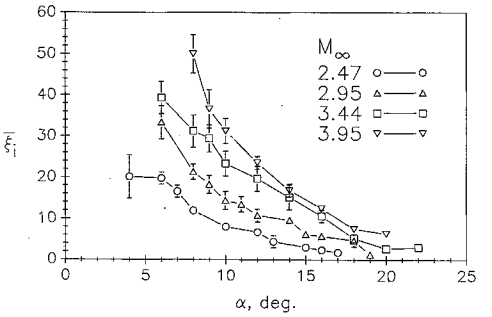

Fig. 4 The trend of the inception length with fin angle.

wave is detached from the shock generator throughout a substantial portion of the boundary layer. This viewpoint was previously stated by Kubota and Stollery for fin interactions.[18]

The inception point was determined as follows. A straight-line asymptote was fitted to the far-field portion of the upstream-influence line. (This also allowed β_U to be determined.[7]) Departure of the asymptote from the actual upstream influence was taken to be the inception point $I(x_i, z_i)$, as can be seen in Fig. 3. The figure also shows the virtual origin V as the intersection of the upstream-influence asymptote and the inviscid shock-wave trace. In practice, the upstream-influence data were replaced by a fourth-order curve fit that smoothed out the data scatter. The criterion for locating I was made objective by setting the fractional departure of the z coordinate from the upstream-influence asymptote to be equal to a small number c_i, i.e.,

$$|z_i - z_{i_{asym}}|/z_i = c_i \tag{7}$$

With c_i = 0.0001, estimates of (x_i, z_i) were not substantially different from the visual estimates in Ref. 15. Either visually or with Eq. (7), $I(x_i, z_i)$ was difficult to locate for weaker interactions, thereby resulting in larger errors. The raw (x_i, z_i) data were then transformed to (ξ_i, ζ_i) coordinates.

Although ξ_i was used in analyzing the inception phenomena, other definitions can be formulated, e.g.,

$$r_i \approx r_v + \xi_i \tag{8}$$

where r_v is the distance from the fin apex to the virtual origin (Fig. 3). The measured lengths are customarily normalized by δ and denoted with overbars; thus, $\bar{\xi}_i = \xi_i/\delta$, etc. In the present study, since Re and δ were fairly constant, the effects of δ or Re_δ could not be explored.

Discussion of Results

Figure 4 is a plot of $\bar{\xi}_i$ against α showing that $\bar{\xi}_i$ decreases as α increases. Thus, at a given Mach number, the inception length decreases as the interaction strength increases. Figure 4 also shows that, for a given α, $\bar{\xi}_i$ increases with Mach number, an observation first noted by Inger.[14]

Previous studies[1,6,7] have shown that α is not an appropriate scaling parameter for fin interactions but have shown that the inviscid shock-wave location plays an important role in characterizing the interaction, as discussed in the Introduction. Therefore, the next step is to examine $\bar{\xi}_i$ against β_0, (Fig. 5). It can be seen that the inception length, to first order, scales with β_0, with a slight decrease in $\bar{\xi}_i$ as M_∞ increases at a fixed β_0. Furthermore, this scaling is nonlinear. When $\beta_0 > 35$ deg, $\bar{\xi}_i$ becomes asymptotically constant and "small," being an order of magnitude less than when $\beta_0 < 25$ deg.

The inception length behavior for $\beta_0 \lesssim 20$ deg could not be explored in the present tests. But, in hypersonic flows, β_0 can easily be smaller than those found in the present tests, e.g., at $M_\infty = 8$, for $\alpha = 5$ deg, $\beta_0 \approx 11$ deg. Care must therefore be exercised in extrapolating the present results to hypersonic

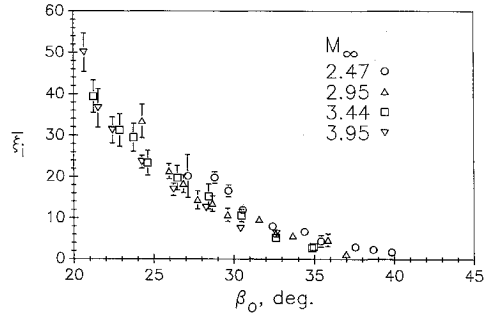

Fig. 5 Scaling of the inception length with shock angle.

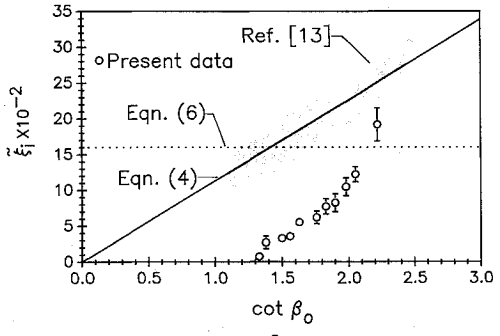

Fig. 6 Scaling of $\bar{\xi}_i$ with cot β_0.

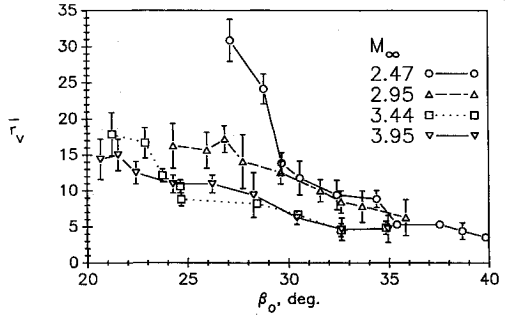

Fig. 7 The virtual origin from the fin apex.

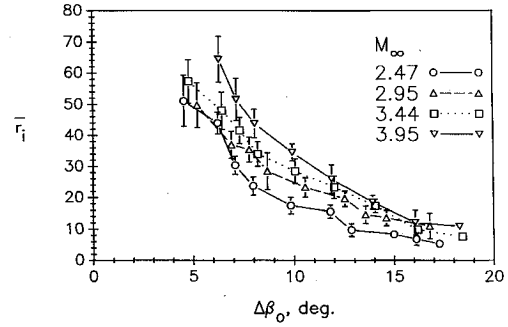

Fig. 8 Inception length scaling by $\Delta\beta_0$.

Mach numbers. Based on the present study, previous measurements of hypersonic fin interactions may have been taken within the inception zone, thus possibly creating discrepancies between supersonic and hypersonic results, e.g., in detecting conical symmetry.[19] Figure 5 shows that at large β_0, there is almost no inception length. In other words, the interaction can be considered to be "fully developed" right from the apex. This has been observed by Zubin and Ostapenko[20] and is also evident in Law's results.[21] Dolling[22] thought that Law's[21] data showed a negligible inception length for all tests (α = 6–16 deg, β_0 = 14–24 deg). However, the inception length can only be crudely estimated using Law's surface pressure data. Furthermore, large inception lengths can give the impression that the interaction is fully developed from the fin apex. As a cautionary note, without systematic explorations of wall temperature and Reynolds number effects, more general conclusions on cold-wall hypersonic data or high Reynolds number data have to be deferred. This study and previous studies[13,14] have only begun to address issues of interaction development and interaction size by accounting for shock sweep.

The present $\bar{\xi}_i$ data also correlate with cot β_0, according to Eq. (4). This can be expected if $\bar{\xi}_i$ scales with β_0 because, in the range 20 deg $\lesssim \beta_0 \lesssim$ 40 deg, cot $\beta_0 \sim 1/\beta_0$. Furthermore, for comparison with data reported by Settles,[13] the present $M_\infty = 2.95$ data are normalized according to Eq. (3) and plotted in Fig. 6. This figure shows that present estimates of $\bar{\xi}_i$ are typically two to three times less than the estimates of Settles, with the disagreement becoming worse as cot β_0 becomes small. The discrepancy is due to different methods in obtaining the inception length. In Ref. 13, the actual upstream-influence line was fitted with a line using a Keuffel & Esser No. 57168548 french curve. The inception point was then located as the intersection between the fitted line and a line parallel to the upstream-influence asymptote and 1 mm inboard. A cross-check using the same french curve showed that, within 5% of ξ_i, estimates of ξ_i are the same between the present results and those of Ref. 13. It is felt that the present method of extracting ξ_i data described previously is more appropriate since there is no reason for the upstream-influence line to be constrained along a prescribed curve. In fact, since the inception and far-field conical regions of the interaction merge gradually, the definition of the inception length is somewhat arbitrary. The key issue is not the criterion itself, as long as it is applied consistently to the entire data set, but the trend of the inception length with Mach number and shock strength.

The Virtual Origin

For completeness and for practical applications,[23,24] the nondimensional distance between the fin apex and the virtual origin $\bar{r}_v$ is plotted against β_0 in Fig. 7. The data scatter tends to be large[25,26] because $\bar{r}_v$ is located by the intersection of two lines separated by a small angle. As also observed in Ref. 25, $\bar{r}_v$ decreases with increasing interaction strength. The present $\bar{r}_v$ data show a weak Mach number dependence when plotted against β_0, similar to the $\bar{\xi}_i$ behavior.

Scaling by $\Delta\beta_0$

The earlier discussion shows the effect of sweep on the inception length development. In addition, to further understand the physical parameters that govern swept interactions, it is necessary to identify shock strength parameters. In Ref. 7 (see Introduction of this article), a reduced shock angle $\Delta\beta_0$ that plays the role of a shock strength parameter was found to scale the reduced upstream-influence angle $\Delta\beta_U$. Therefore, the question arises whether the inception zone can be scaled by $\Delta\beta_0$. Bearing in mind that the polar coordinate system is centered at the virtual origin and not at the fin apex, the $\bar{\xi}_i$ data must be corrected to $\bar{r}_i$ according to Eq. (8).[27,28] A plot of $\bar{r}_i$ against $\Delta\beta_0$ (Fig. 8) shows satisfactory collapse of the data, thereby identifying the appropriateness of $\Delta\beta_0$ in scaling the

inception length. There is a slight Mach number trend to the data as expected if the previously formulated scaling of $\Delta\beta_U$ by $\Delta\beta_0$ is to be valid.

Conclusions

The inception length to conical symmetry for fin-generated shock-wave boundary-layer interactions was found to be weakly dependent on Mach number and to depend strongly on shock sweep. The inception length was found to be constant and small for shock angles larger than about 35 deg. Otherwise, the inception length was found to increase with decreasing shock angle. A previously formulated shock strength parameter was found to scale the inception length approximately.

Acknowledgments

The experimental work reported in this paper was done by the first author during his Ph.D. research at the Gas Dynamics Laboratory, Pennsylvania State University. It was supported by AFOSR Grant 86-0082 from the U.S. Air Force Office of Scientific Research, monitored by L. Sakell, and by Joint Research Interchange NCA2-192 with the NASA Ames Research Center in which C. C. Horstman was the research collaborator. The preparation of this paper was partly supported by NASA-Langley through Grant NAG 1-891 monitored by J. P. Weidner. The authors acknowledge the comments of D. S. Dolling, the University of Texas at Austin, and of the reviewers.

References

[1]Settles, G. S., and Dolling, D. S., "Swept Shock Wave/Boundary-Layer Interactions," *Tactile Missile Aerodynamics,* Vol. 104, edited by M. J. Hemsch and J. N. Nielsen, *Progress in Astronautics and Aeronautics,* AIAA, Washington, D.C., pp. 297–379.

[2]Settles, G. S., and Dolling, D. S., "Swept Shock/Boundary-Layer Interactions—Tutorial and Update," AIAA Paper 90-0375, Jan. 1990.

[3]Settles, G. S., and Teng, H.-Y., "Flow Visualization Methods for Separated Three-Dimensional Shock Wave/Turbulent Boundary-Layer Interactions," *AIAA Journal,* Vol. 21, No. 3, 1983, pp. 390–397.

[4]Lu, F. K., and Settles, G. S., "Color Surface-Flow Visualization of Fin-Generated Shock-Wave Boundary-Layer Interactions," *Experiments in Fluids,* Vol. 8, 1990, pp. 352–354.

[5]Settles, G. S., and Teng, H.-Y., "Cylindrical and Conical Flow Regimes of Three-Dimensional Shock/Boundary-Layer Interactions," *AIAA Journal,* Vol. 22, No. 2, 1985, pp. 194–200.

[6]Settles, G. S., and Lu, F. K., "Conical Similarity of Shock/Boundary-Layer Interactions Generated by Swept and Unswept Fins," *AIAA Journal,* Vol. 23, No. 7, 1985, pp. 1021–1027.

[7]Lu, F. K., Settles, G. S., and Horstman, C. C., "Mach Number Effects on Conical Surface Features of Swept Shock Boundary-Layer Interactions," *AIAA Journal,* Vol. 28, No. 1, 1990, pp. 91–97.

[8]Token, K. H., "Heat Transfer due to Shock Wave Turbulent Boundary Layer Interactions on High Speed Weapon Systems," Air Force Flight Dynamics Laboratory, Wright-Patterson AFB, AFFDL-TR-74-77, April 1974.

[9]Peake, D. J., "The Three-Dimensional Interaction of a Swept Shock Wave with a Turbulent Boundary Layer and the Effects of Air Injection on Separation," Ph.D. dissertation, Carleton Univ., Ottawa, Canada, 1975.

[10]Dolling, D. S., and Bogdonoff, S. M., "Upstream Influence in Sharp Fin-Induced Shock Wave Turbulent Boundary-Layer Interaction," *AIAA Journal,* Vol. 21, No. 1, 1983, pp. 143–145.

[11]Settles, G. S., and Bogdonoff, S. M., "Scaling of Two- and Three-Dimensional Shock/Turbulent Boundary-Layer Interactions at Compression Corners," *AIAA Journal,* Vol. 20, No. 6, 1982, pp. 782–789.

[12]Lu, F. K., and Settles, G. S., "Upstream-Influence Scaling of Fin-Generated Shock Wave Boundary-Layer Interactions," AIAA Paper 90-0376, Jan. 1990.

[13]Settles, G. S., "On the Inception Lengths of Swept Shock-Wave/Turbulent Boundary-Layer Interactions," *Proceedings of the IUTAM Symposium on Turbulent Shear-Layer/Shock-Wave Interactions,* edited by J. Délery, Springer-Verlag, Berlin, 1986, pp. 203–213.

[14]Inger, G. R., "Spanwise Propagation of Upstream Influence in Conical Swept Shock/Boundary-Layer Interactions," *AIAA Journal,* Vol. 25, No. 2, 1987, pp. 287–293.

[15]Lu, F. K., "Fin Generated Shock-Wave Boundary-Layer Interactions," Ph.D. dissertation, The Pennsylvania State Univ., University Park, PA, 1988.

[16]Stalker, R. J., "Viscous Effects in Supersonic Flow," Ph.D. dissertation, Univ. of Sydney, Sydney, Australia, 1959.

[17]Özcan, O., and Kaya, M. O., "Shock-Wave/Boundary-Layer Interactions at a Swept Compression Corner," *AIAA Journal,* Vol. 27, No. 11, 1989, pp. 1646–1648.

[18]Kubota, H., and Stollery, J. L., "An Experimental Study of the Interaction Between a Glancing Shock Wave and a Turbulent Boundary Layer," *Journal of Fluid Mechanics,* Vol. 116, 1982, pp. 431–458.

[19]Holden, M. S., "Experimental Studies of Quasi-Two-Dimensional and Three-Dimensional Viscous Interaction Regions Induced by Skewed-Shock and Swept-Shock Boundary-Layer Interaction," AIAA Paper 84-1677, June 1984.

[20]Zubin, M. A., and Ostapenko, N. A., "Structure of Flow in the Separation Region Resulting from Interaction of a Normal Shock Wave with a Boundary Layer in a Corner," *Izv. Akad. Nauk SSSR, Mekh. Zhid. i Gaza,* Vol. 14, 1979, pp. 51–58, (Engl. trans.).

[21]Law, C. H., "Three-Dimensional Shock Wave-Turbulent Boundary Layer Interactions at Mach 6," ARL-TR-75-0191, Aerospace Research Laboratories, Wright-Patterson AFB, 1975.

[22]Dolling, D. S., "Upstream Influence in Conically Symmetric Flow," *AIAA Journal,* Vol. 23, No. 6, 1985, pp. 967–969.

[23]Hsu, J. C., and Settles, G. S., "Measurements of Swept Shock Wave/Turbulent Boundary-Layer Interactions by Holographic Interferometry," AIAA Paper 89-1849, June 1989.

[24]Alvi, F. S., and Settles, G. S., "A Parametric Study of Swept Shock Wave/Turbulent Boundary-Layer Interaction Structures Using White-Light Conical Shadowgraphy," AIAA Paper 90-1644, June 1990.

[25]Lu, F. K., "An Experimental Study of Three-Dimensional Shock Wave Boundary Layer Interactions Generated by Sharp Fins," M.S.E. thesis, Princeton Univ., Princeton, NJ, 1983.

[26]Kimmel, R. L., "An Experimental Investigation of Quasi-Conical Shock Wave/Turbulent Boundary Layer Interactions," Ph.D. dissertation, Princeton Univ., Princeton, NJ, 1987.

[27]Lu, F. K., and Settles, G. S., "Structure of Fin-Shock/Boundary-Layer Interactions by Laser Light-Screen Visualization," AIAA Paper 88-3801, July 1988.

[28]Lu, F. K., and Settles, G. S., "Inception Length to a Fully-Developed Fin-Generated Shock Wave Boundary-Layer Interaction," AIAA Paper 89-1850, June 1989.